

Fabrication and characterization of TiO₂ nanoparticles conjugated luminescence upconversion nanoparticles

Seda Demirel Topel^{1*}, Önder Topel², Günseli Turgut Cin²

¹Department of Material Science and Nanotechnology Engineering, Faculty of Engineering, Antalya Bilim University, 07190, Antalya, Turkey

²Department of Chemistry, Faculty of Science, Akdeniz University, 07058 Antalya, Turkey

*corresponding author e-mail address: seda.demireltopel@antalya.edu.tr

ABSTRACT

TiO₂ nanoparticles conjugated luminescence upconversion (TiO₂-UC) nanocomposites have been fabricated by covalently linking of carboxyl-functionalized TiO₂ and amino-functionalized NaYF₄:Yb³⁺,Er³⁺,Ce³⁺ upconversion nanoparticles (UCNP) in the presence of *N,N'*-dicyclohexylcarbodiimide (DCC) /4-dimethylaminopyridine (DMAP) coupling reagents. The carboxyl-functionalized TiO₂ nanoparticles and amino-functionalized UCNPs have been synthesized by hydrothermal method with 5±2 and 55±10 nm in diameter, respectively. In the synthesis of UCNPs, the percentage of stabilizing agent (polyethyleneimine, PEI), the mole ratios of NaCl/NH₄F and the co-doping ratio of Ce³⁺ ion have been found to be a significant effect on their size and morphology. Size, morphology, conjugation as well as photo-physical properties of all synthesized nanomaterials have been characterized by means of X-ray diffraction (XRD), transmission electron microscopy (TEM), Fourier transform infrared spectroscopy (FTIR), X-ray photoelectron spectroscopy (XPS), and fluorescence spectroscopy. UCNPs and TiO₂-UC nanocomposites exhibit strong green luminescence at room temperature under 980 nm excitation led the emissions at 440, 520, 540 and 658 nm, representing ²H_{9/2} → ⁴I_{15/2}, ²H_{11/2} → ⁴I_{15/2}, ⁴S_{3/2} → ⁴I_{15/2} and ⁴F → ⁴I_{15/2} transitions, respectively. The water dispersible luminescence nanocomposites having NIR light utilizing ability are promising for efficient light harvesting and/or bio-imaging applications.

Keywords: upconversion; rare earths; TiO₂ nanoparticles; luminescence; water soluble.

1. INTRODUCTION

Upconversion is a non-linear optical process generating higher energy emission from low-energy radiation and especially upconversion near infrared light (NIR) to the visible light has been of special interest since Auzel, Ovsyankin and Feodilov in the 1960s was firstly reported this concept [1, 2, 3]. Lanthanide-doped NaREF₄ (RE:rare earth) upconversion nanoparticles (UCNPs) are one of the most important upconversion materials, and have been subject to many applications such as biological labeling [4, 5, 6], photodynamic therapy [7, 8], drug delivery [9, 10], dye sensitized solar cells [11, 12], 3D optical displays [13, 14], security labeling [15, 16] and optical storage [17] in the last decades. Generally, the UCNPs consist of a host lattice and doped lanthanide ions in which may act as an absorber and emitter ion in the host lattice material. Some crystalline lattices of trivalent rare earth ions (Sc³⁺, Y³⁺, La³⁺, Gd³⁺), alkaline earth ions (Ca²⁺, Sr²⁺, Ba²⁺) or certain transition metals (Ti⁴⁺, Zr⁴⁺) may be used as the host materials [18]. The most commonly used hosts are halides (NaYF₄, YF₃, LaF₃), oxides (Y₂O₃, ZrO₂) and oxysulfides (Y₂O₂S, La₂O₂S) [19]. On the other hand, the dopant ions located in the selected host lattice play a critical role for absorbing (e.g. Yb³⁺) and emitting photons (Er³⁺, Tm³⁺, Ho³⁺) which are responsible for the colour of emitted light [20]. Many lanthanide ions (Ln³⁺) have metastable intermediate electronic states to be able to generate an upconversion emission. The shielding of the 4f electrons of Ln³⁺ by completely filled 5s² and 5p⁶ sub-shells results in a weak electron-phonon coupling that exhibits sharp and narrow *f-f*

transition bands and forbidden *f-f* transitions arising long-lived excited states (up to 100 ms) [18, 21].

In order to synthesize UCNPs, a variety of chemical synthesis methods including co-precipitation [22], thermal decomposition [23], hydro(solvo)thermal synthesis [24] and sol-gel [25], have been applied. In each of these techniques, optimization of synthesis parameters in the method is crucial to obtain nanocrystals having desired size, morphology, and optical properties. The surfaces of UCNPs have also been modified with nanoparticles, small molecules and polymers in order to have different properties in the literature. For example, TiO₂ nanoparticles have been coated on UCNPs especially for the following purposes: *i*) to build up a dye sensitized solar cell (DSSC) improved light harvesting ability to NIR region with UCNPs [26] and *ii*) to fabricate a NIR-responsive photo-catalyst. Conventional DSSCs can work well in the visible region even though they cannot harvest NIR part of sunlight effectively. For more efficiently utilization of solar spectrum in maximum range of energy, new type dyes and quantum dots in DSSCs having ability harvesting the NIR region of polychromatic solar spectrum are currently under development [27]. Regarding this, it is obvious that UCNPs are a potential candidate to extend the energy absorbing range. Demopoulos and co-workers synthesized TiO₂ combined UCNPs (LaF₃:Yb/Er) in 2010 [28] for the first time and found that Er³⁺,Yb³⁺ co-doped LaF₃ part of the nanomaterial captures NIR light and converts it into visible light absorbable by

a dye which opens up a new approach for the development of DSSCs having higher conversion efficiency and photocurrent output [28]. After that Fu and co-workers improved the efficiencies of the solar cells by adding graphene to the TiO₂-UC (NaYF₄:Yb³⁺,Er³⁺) nanocomposites in 2012 [29]. On the other hand, due to the photocatalytic properties of TiO₂ nanoparticles, TiO₂-UC nanocomposites are assessed as a NIR-responsive photocatalyst. In 2013, Qin and co-workers produced core-shell structured nanoparticles (NaYF₄:Yb³⁺,Tm³⁺@TiO₂) to investigate the photocatalytic activity on methylene blue as a model molecule [30]. Their results show that energy transfer route between NaYF₄:Yb³⁺,Tm³⁺ and TiO₂ is an important factor to affect the photocatalytic activity, and oxidation of reactive oxygen species (ROS) generated in the photocatalytic reaction is mainly responsible for degradation of organic pollutants under NIR irradiation. Furthermore, the ROS generated by TiO₂-UC nanocomposites under NIR light might be used for killing the cancer cells by photodynamic therapy (PDT). In 2015, Zhang and co-workers produced core-shell structured TiO₂-

NaYF₄:Yb³⁺,Tm³⁺ nanocomposites and covered by PEG (polyethylene glycol) to prevent their aggregation in biological environment [31-34]. They applied the UC nanocomposites to test their PDT efficiencies and showed that PEGylated NaYF₄:Yb³⁺,Tm³⁺-TiO₂ under 980 nm NIR laser kills cancer cells both *in vitro* and *in vivo*. In the applications mentioned above and also in recent studies [31, 32, 33, 34], TiO₂ have been coated on the UCNPs by means of hydrolysis of titanium alkoxide precursor in ethanol in the presence of base at UCNP surface. To our knowledge, there is no report on the covalently conjugation of TiO₂ nanoparticles on Ce³⁺ co-doped NaYF₄:Yb³⁺, Er³⁺ UCNPs. We present a covalent conjugation of the citrate coated TiO₂ nanoparticles to the PEI coated NaYF₄:Yb³⁺,Er³⁺,Ce³⁺ UCNPs in the presence of *N,N'*-dicyclohexylcarbodiimide (DCC) /4-dimethylaminopyridine (DMAP) coupling reagents and Ce³⁺ doping effect on UCNPs in this study. Introducing the TiO₂ nanoparticles on the UCNPs surface increases the water dispersibility of UCNPs which might enhance the light harvesting efficiency as well as open up new biomedical applications.

2. EXPERIMENTAL SECTION

2.1. Materials.

Rare-earth chlorides (RECl₃.xH₂O, 99.99%), sodium chloride (NaCl), sodium hydroxide (NaOH), ammonium fluoride (NH₄F), polyethyleneimine (PEI, branched polymer, MW:10.000), titanium(IV)isopropoxide (Ti(OPrⁱ)₄), citric acid monohydrate *N,N'*-dicyclohexylcarbodiimide (DCC), 4-dimethylaminopyridine (DMAP) and all solvents were analytical grade, purchased from Sigma-Aldrich and used without further purification.

2.2. Synthesis of PEI coated NaYF₄:Yb³⁺, Er³⁺,Ce³⁺ upconversion nanoparticles.

Upconversion nanoparticles with the following composition, NaYF₄(72%), Yb³⁺ (20%), Er³⁺ (5%), Ce³⁺ (3%) were prepared via hydrothermal method. In a 100 mL teflon beaker, YCl₃.6H₂O (140.59 mg, 0.72 mmol), YbCl₃.6H₂O (55.58 mg, 0.2 mmol), ErCl₃.6H₂O (13.68 mg, 0.05 mmol), CeCl₃.6H₂O (7.39 mg, 0.03 mmol) and NaCl (58.44 mg, 1 mmol) were dissolved in 4 mL ultrapure water (dd.H₂O). 50 mL ethanol were added to the solution and stirred for 5 min. To this solution, 10 ml of PEI (MW: 10.000g/mol) solution (1 g PEI in 20 mL dd.H₂O) and NH₄F (185.2 mg, 5 mmol) was added, and then the teflon beaker was placed to autoclave and heated up 200°C for 3h. The separated UCNPs by centrifuging at 8500 rpm for 15 min were washed with ethanol:water (10:10 mL) mixture for 3 times and then dried in a vacuum oven at 40°C [35].

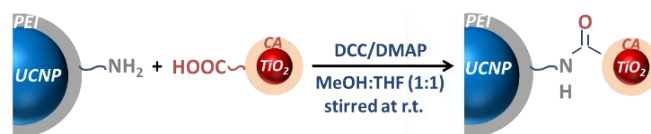
2.3. Synthesis of citrate coated TiO₂ nanoparticles.

Ti(OPrⁱ)₄ (2.32 g, 8.2 mmol) was dissolved in 47 mL of *n*-propanol a 100 mL teflon beaker at ambient temperature. After 10 min stirring, *n*-propanol/hydrochloric acid mixture was added dropwise into alkoxide solution using a burette with very slow rate. The solution was left for additional 10 min stirring. Then water/*n*-propanol mixture was added into the solution in the same rate and stirred at ambient temperature for 30 min. Teflon beaker containing final mixture was placed in a hydrothermal reactor and heated at 150°C for 2 h. The mole ratio of H₂O/Ti(OPrⁱ)₄ and

HCl/Ti(OPrⁱ)₄ were 2 and 0.2, respectively. At the end of the time, the mixture cooled down to room temperature, TiO₂ nanoparticles were then separated through centrifugation at 8500 rpm and dried in a vacuum oven at 30°C for 4 h [36]. In order for citric acid coating on the surface of nanoparticles, TiO₂ nanoparticles (149 mg, 1.87 mmol) were dispersed in dd. H₂O (100 mL) and then citric acid monohydrate (1.96 g, 9.35 mmol) was added to the dispersion. The pH of the mixture was adjusted at 10 by adding NaOH (0.1M) and then heated at 55°C for 2 hours. After cooling down the reaction mixture to room temperature, the citrate coated TiO₂ nanoparticles were separated by centrifuge at 8500 rpm for 15 min and dried in a vacuum oven at 40°C [37].

2.4. Synthesis of TiO₂ conjugated NaYF₄:Yb³⁺, Er³⁺,Ce³⁺ upconversion (TiO₂-UC) nanocomposites.

The synthesis route of the conjugation of TiO₂ and NaYF₄:Yb³⁺, Er³⁺, Ce³⁺ upconversion nanoparticles through DCC/DMAP coupling chemistry used in this study is illustrated in Scheme 1. In a 50 mL round bottom flask, citrate functionalized TiO₂ (10 mg) were dispersed in MeOH:THF (1:1) solution under nitrogen atmosphere. PEI functionalized upconversion nanoparticles (50 mg), DCC (2.9 mg, 0.014 mmol) and DMAP (0.17 mg, 1.4.10⁻³ mmol) reagents were added to the TiO₂ solution. The reaction mixture was stirred at room temperature under nitrogen atmosphere overnight. TiO₂-UC nanocomposites were separated via centrifuge at 8500 rpm for 15 min, and then washed with 10 mL of ethanol:water (1:1) mixture for 3 times and dried in vacuum oven at 40°C.



Scheme 1. Synthetic route for TiO₂-UC nanocomposites.

2.5. Characterization.

The morphology and size of the prepared nanoparticles were characterized by a transmission electron microscope (TEM) (FEI tecnai G2 F30) using an accelerating voltage of 200keV. A small drop of nanoparticle dispersions was put on a 50 Å thick carbon-coated copper grid (300 mesh) then the excess solution was immediately removed. Powder XRD measurements were performed at room temperature (Rigaku, micromax 007HFDW)

3. RESULTS SECTION

We used the hydrothermal method to synthesize UCNPs which is a water-based system providing a relatively green method compared to other synthesis techniques such as thermal decomposition and co-precipitation required toxic precursors and harsh reaction conditions [13,14]. The parameters such as solvent amount, PEI ratio, NaCl/NH₄F ratio and Ce³⁺ ion co-doping ratios etc. have been optimized in order to obtain uniform UCNPs with small size and hexagonal phase, since luminescence performance of UCNPs having hexagonal phase is 10 times more than cubic phase [38]. The results from optimization studies are given in Table 1. To be able to adjust the size and the crystal phase, we use Ce³⁺ doping in the experiments 4, 5 and 6 and found that introducing Ce³⁺ ion in the upconversion nanocrystal structure together with increasing PEI % and volume of the solvent has led to decrease the size of UCNPs in hexagonal phase (Table 1). Wang and co-workers explained this Ce³⁺ ion doping effect on the host lattice (NaYF₄) referring the system free energy and anisotropic crystal growth: ‘doping a larger ion like Ce³⁺ can decrease the energy barrier and lead to hexagonal phase UCNPs’ [39]. We chose the UCNPs from the experiment 6 for further studies since the attempt resulted in more uniform and smaller size UCNPs, even though it yielded a mixture of hexagonal and cubic phase (Table 1).

Table 1. Reaction conditions for the synthesis of PEI coated UCNPs.

No	RE ³⁺ mole ratios (%) Y : Yb : Er : Ce	NaCl:NH ₄ F (mole ratio)	PEI %	Method	Solvent (mL)	Temp. (°C)	Time (h)	Crystal phase	Size
1	80:18:2:--	1: 2	2.25	teflon beaker (open air)	EG (40 mL)	200	24	Cubic	~60 nm
2	80:18:2:--	1:2	2.25	sealed tube	EG (40 mL)	200	24	Cubic	~35 nm
3	80:18:2:--	1:5	2.25	hydrothermal	H ₂ O/EtOH (10 mL)	200	3	hexagonal cubic	~3 μm ~100 nm
4	72:20:5:3 (C _{total} =0.5 M)	1: 5	5	hydrothermal	H ₂ O/EtOH (20 mL)	200	3	hexagonal cubic	~2 μm ~100 nm
5	72:20:5:3 (C _{total} =0.5 M)	1: 5	5	hydrothermal	H ₂ O/EtOH (30 mL)	200	3	hexagonal cubic	~200 nm ~65 nm
6	72:20:5:3 (C _{total} =0.5 M)	1: 5	5	hydrothermal	H ₂ O/EtOH (50 mL)	200	3	hexagonal cubic	55 nm

The size and morphology of the synthesized PEI coated UCNPs were also investigated by TEM measurements. Figure 1 (A-D) represents the typical TEM images of UCNPs that are particularly well distributed in size, but it seems that the nanoparticles tend to be agglomerated due to the preparation of the sample in water solution (Fig. 1A and 1C). The histogram shows that the average particle size of PEI coated UCNPs is 55±10 nm in diameter determined from the TEM images with Adobe Photoshop 7 by counting 145 nanoparticles (Fig. 1B). The selected area electron diffraction (SAED) pattern shows NaYF₄ lattice to have well crystallinity (Fig 1E).

Citrate coated TiO₂ nanoparticles for surface conjugation of UCNPs were synthesized by hydrothermal method. TEM

by using Cu-Kα (1.5418 Å) radiation. X-ray photoelectron spectrometer (XPS) analysis was carried out on Thermo Scientific, K-alpha. Fourier transform infrared spectroscopy (FTIR) spectra were recorded on a Bruker Tensor 27 spectrometer. The PL spectra were obtained with a confocal Raman spectrometer (Wited, Alpha 300S) by using external NIR continuous wave (CW) laser light (50 mW, 980 nm). All measurements were performed at room temperature.

images of citrate coated TiO₂ nanoparticles are shown in Fig 2. The particles were fabricated so as to be spherical and highly monodisperse with an average diameter of 5±2 nm (Fig. 2A-C). Their size and size distribution were determined by sizing the particles in the TEM images with Adobe Photoshop 7. Total of 233 nanoparticles were counted and averaged. Selected area electron diffraction (SAED) pattern is also clearly indicated that synthesized TiO₂ nanoparticles are highly crystalline phase (Fig. 2D).

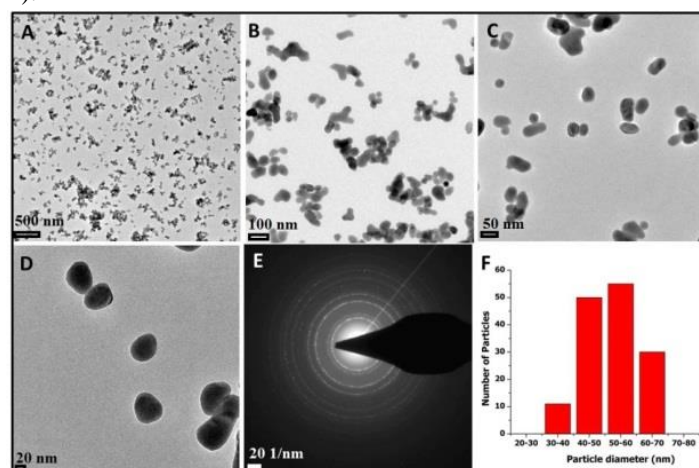


Fig. 1. TEM images (A-D) and size distribution (F) of PEI coated NaYF₄:Yb³⁺, Er³⁺, Ce³⁺ UCNPs (the scale bars for A-D is 500, 100, 50 and 20 nm, respectively). The image E shows selected-area electron diffraction (SAED) pattern of NaYF₄ lattice.

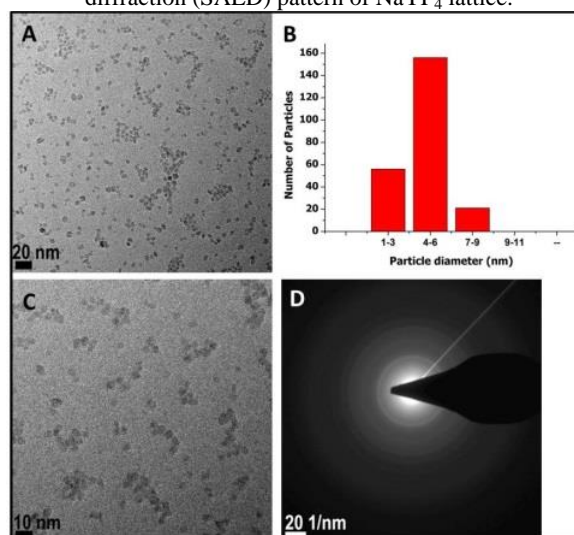


Fig. 2. TEM images and size distribution of citrate coated TiO₂ nanoparticles, (A, B and C). The image D shows selected-area electron diffraction (SAED) pattern of citrate coated TiO₂ nanoparticles.

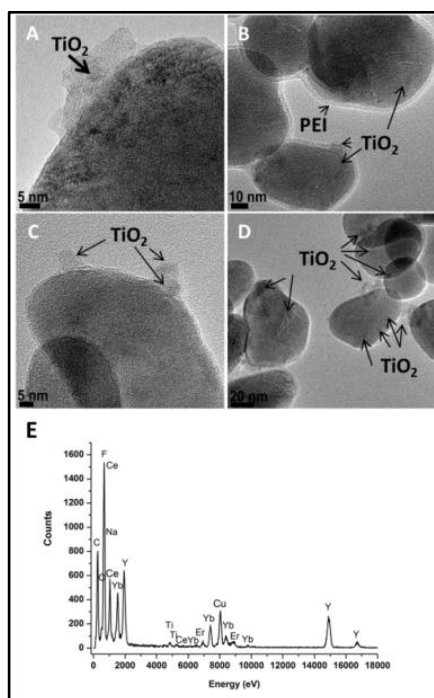


Fig. 3. TEM images (A–D) and TEM–EDX analysis (E) of TiO₂–UC nanocomposites.

The synthesized citrate coated TiO₂ nanoparticles were covalently conjugated on the surface of PEI coated NaYF₄:Yb³⁺,Er³⁺,Ce³⁺ upconversion nanoparticles through DCC/DMAP coupling reaction to fabricate TiO₂–UC nanocomposites. Representative TEM images of the resultant TiO₂–UC nanocomposites are given in Fig. 3. It can be clearly seen from Fig 3(A–D) there are not any free TiO₂ nanoparticles on the grid and all of the TiO₂ nanoparticles were attached on the surface of UCNPs. There is no change in their individual sizes of previously prepared citrate coated TiO₂ and PEI coated UCNPs after bonding. An energy-dispersive X-ray (EDX) spectrum of TiO₂–UC nanocomposites shows to be strong peaks belonging Y, F atoms and relatively weaker peaks belonging Yb, Na, Er, Ce and Ti atoms which proves the existence of NaYF₄ and TiO₂ in the TiO₂–UC nanocomposite.

Crystal structures of the synthesized nanoparticles were characterized by means of X-ray powder diffraction measurements. Fig. 4a–c shows the diffraction patterns of citrate coated TiO₂ nanoparticles, TiO₂–UC nanocomposites and PEI coated UCNPs (NaYF₄:Yb³⁺, Er³⁺, Ce³⁺). According to Joint Committee on Powder Diffraction Standards (JCPD), the synthesized PEI–UCNPs represent a mixture of α -cubic (JCPDS27–0697) and β -hexagonal (JCPDS27-0698) crystal phases [23] whereas citrate coated TiO₂ nanoparticles are purely in anatase phase (JCPDS 21-1272) [40].

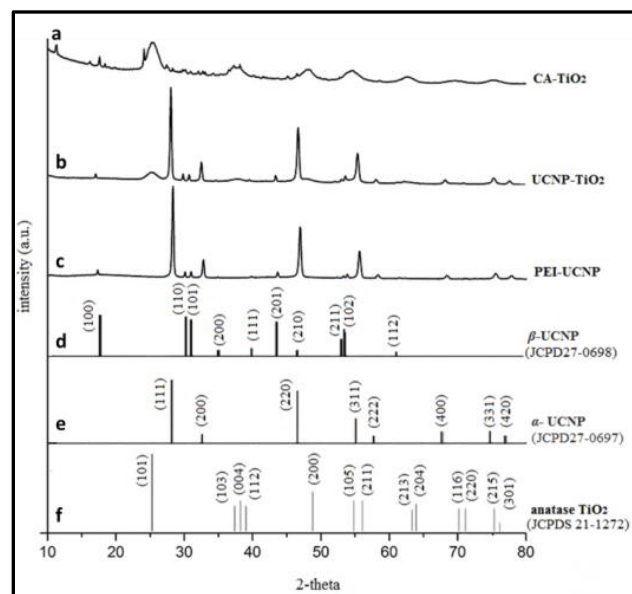


Fig. 4. XRD pattern of CA–TiO₂ NPs (a), TiO₂–UCNP (b), PEI–UCNP (c). The corresponding reference data from JCPDS for β – α –UCNP and anatase TiO₂ (d–f), respectively.

Covalent conjugation between PEI coated UCNPs and citric acid functionalized TiO₂ nanoparticles was proved by FTIR and XPS measurements. Fig. 5 shows the FTIR spectra of (a) PEI functionalized UCNP, (b) TiO₂–UC nanocomposites and (c) citrate functionalized TiO₂ NPs, respectively. N–H bending and C–N stretching vibrations observed at 1611 and 1069 cm⁻¹, respectively in Fig. 5a, represent free amine groups in PEI coated UCNPs confirming the existence of PEI on the UCNPs surface together with the stretching bands of alkyl chain in PEI arising at 2944 and 2847 cm⁻¹. The citrate coated TiO₂ particles have the characteristic vibrations at 611 cm⁻¹ due to stretching bands of Ti–O–Ti (Fig. 5c). The two prominent bands belonging to deprotonated citrate ions (carboxylate group), 1569 and 1375 cm⁻¹, are assigned to the asymmetric and symmetric stretching motions of carboxylate group, respectively (Fig. 5c). The stretching vibration of C–O group is also appeared at 1097 cm⁻¹. The broad bands observed at 3402 and 3222 cm⁻¹ are attributed to O–H stretching vibrations of water adsorbed to the surface of CA coated TiO₂ nanoparticles (Fig 5c). After covalently binding of citrate functionalized TiO₂ nanoparticles to PEI modified UCNPs, new stretching peaks arise at 1625 (C=O, amide–I), 1558 (N–H, amide–II) and 1375 cm⁻¹ (C–N, amide–III) due to the amide formation in the resultant UC nanocomposites (Fig. 5b). The characteristic N–H stretching vibration belonging to amide group is also appeared at 3333 cm⁻¹ (Fig. 5b).

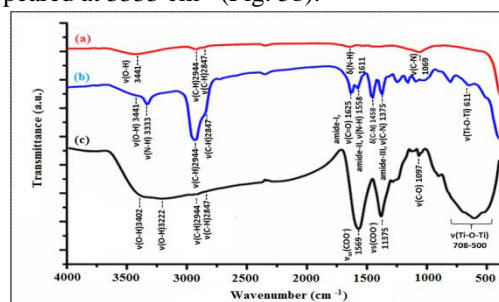


Fig. 5. FTIR spectra of PEI functionalized UCNPs (a), TiO₂–UC nanocomposite (b) and citrate functionalized TiO₂ NPs (c).

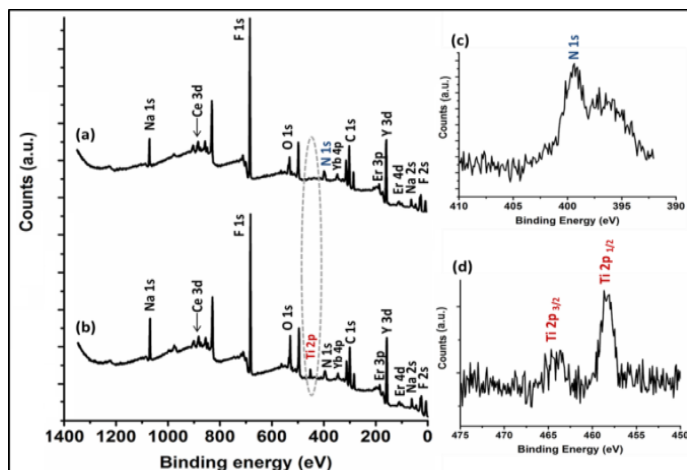


Fig. 6. XPS survey spectra of PEI coated UCNP, TiO₂-UC nanocomposites, respectively (a,b). The focused spectra on N1s and Ti2p binding energy regions are seen in (c,d), respectively.

To further characterize chemical composition and relevant surface chemistry of PEI coated UCNPs and TiO₂-UC nanocomposites, XPS measurements were performed in the range of 0–1350 eV (Fig. 6). The peaks corresponding to the binding energy of host elements Y (Y 3p_{3/2}, 316 eV; Y 3p_{3/2}, 301 eV; 3d_{5/2}, 165 eV), Na (1s, 1075 eV), F (1s, 688 eV) and dopants Yb (4d, 190 eV), Er (4d, 150 eV) and Ce (3d, 929 eV) are seen obviously in XPS spectra in Fig. 6a. Carbon 1s signal at 288 eV is due to the carbon used for the calibration. The peak at 402 eV corresponding to N1s confirms the existence of PEI on PEI functionalized UCNPs. New arising peaks at 458 eV (Ti 2p_{1/2}) and 463 eV (Ti 2p_{3/2}) indicates the binding TiO₂ nanoparticles to the UCNPs surface (Fig 6b,d) which supports the results from FTIR measurements in Fig.5.

4. CONCLUSIONS

TiO₂ and upconversion (UC) nanoparticles were individually synthesized by hydrothermal method with an average size of 5±2 nm and 55±5 nm with a narrow size distribution. Both TiO₂ and UC nanoparticles were obtained in high crystallinity with anatase and hexagonal-cubic phase, respectively. To introduce the PEI and Ce³⁺ ion into upconversion nanocrystals resulted in uniform and small nanoparticles having a mixture of cubic-hexagonal phase. TiO₂ nanoparticles were conjugated to

5. REFERENCES

- [1] Auzel F., Computer quantique par transfert d'energie entre deux ions de terres rares dans un tungstate mixte et dans un verre, *C.R. Acad. Sci. Paris*, 262, 1016-1019, **1966**.
- [2] Ovsyankin V.V., Feofilov P.P., On the mechanism of adding of electronic excitations in doped crystals, *Sov. Phys. JETP Lett.*, 3, 322-323, **1966**.
- [3] Riuttamäki T., Soukka T., Upconverting Phosphor Labels for Bioanalytical Assays, *Advances in chemical bioanalysis. Bioanalytical Reviews*, 1, Springer, Cham, 155-204, **2013**.
- [4] Wang F., Banerjee D., Liu, Y., Chen X., Liu X., Upconversion nanoparticles in biological labeling, imaging, and therapy, *Analyst*, 135, 1839-1854, **2010**.
- [5] Duan C., Liang L., Li L., Zhaang R., Xu Z.P., Recent progress in upconversion applications, *Journal of Materials Chemistry B*, 6, 192-209,

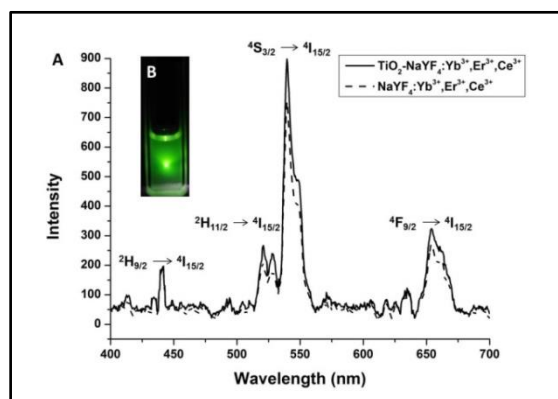


Fig. 7. Fluorescent spectra of the UCNP and TiO₂-NaYF₄:Yb³⁺,Er³⁺,Ce³⁺ nanocomposites under 50 mW, 980 nm CW laser (A). Inset B: photo of UCNP solution (1 mg/mL) in water:ethanol (1 :1) under 980 nm laser at room temperature

Luminescence spectra of NaYF₄:Yb³⁺, Er³⁺, Ce³⁺ UCNPs and the TiO₂-UC nanocomposites at the room temperature given in Fig. 7 shows the narrow emission bands corresponding to characteristic *4f-4f* transitions of Er³⁺ ions doped in the UCNPs. The green emission observed at 440, 520 and 540 nm originate from ²H_{9/2} → ⁴I_{15/2}, ²H_{11/2} → ⁴I_{15/2}, ⁴S_{3/2} → ⁴I_{15/2} transition, respectively, whereas the red fluorescence at 658 nm is attributed to the ⁴F_{9/2} → ⁴I_{15/2} transition [41]. After the attachment of TiO₂ nanoparticles, the emission intensity is seen to be a slightly enhanced compared to bare UCNPs (see Fig. 7). The photostability of the synthesized TiO₂-UC nanocomposites in water was tested by continually exposing a dispersion of TiO₂-UC nanocomposites in water to a 980 nm focused laser for over 1 hour and it was not observed any damping in emission intensity which means TiO₂-UC nanocomposites to have good photo-stability in water.

NaYF₄:Yb³⁺,Er³⁺,Ce³⁺ UCNPs *via* covalent coupling reaction. The prepared TiO₂-UC nanocomposites are highly monodisperse and show a good photo-stability in water. They show slightly improved emission intensity in comparison to bare UCNPs under the excitation of 980 nm after the conjugation with TiO₂ nanoparticles. Developed multifunctional nanocomposites are promising for both light harvesting applications and biomedical applications.

- [6] Wilhem S., Perspectives for upconverting nanoparticle, *ACS Nano*, 11, 10644-10653, **2017**.
- [7] Idris N.M., Gnanasammandhan M.K., Zhang J., Ho P.C., Mahendran R., Zhang Y., In vivo photodynamic therapy using upconversion nanoparticles as remote-controlled nanotransducers, *Nature Medicine*, 18,1580-1585, **2012**.
- [8] Fan W., Bu W., Shi J., On the latest three stage development of nanomedicines based on upconversion nanoparticles, *Advanced Materials*, 28, 3987-4011, **2016**.
- [9] Wang C., Cheng L., Liu Z., Drug delivery with upconversion nanoparticles for multi-functional targeted cancer cell imaging and therapy, *Biomaterials*, 32, 1110-1120, **2011**.
- [10] Chin A.L., Zhong Y., Tong R., Emerging strategies in near-infrared

- light triggered drug delivery using organic nanomaterials, *Biomaterial Sciences*, 5, 1491-1499, **2017**.
- [11] Zou W., Visser C.J., Maduro A., Pshenichnikov M.S., Hummelen J.C., Broadband dye sensitized upconversion of near infrared light, *Nature Photonics*, 6, 560-564, **2012**.
- [12] Wang X., Valiev R.R., Ohulchanskyy T.Y., Ången H., Yang C., Chen G., Dye-sensitized lanthanide-doped upconversion nanoparticles, *Chemical Society Reviews*, 26, 4150-4167, **2017**.
- [13] Downing E., Hesselink L., Ralston J., Macfarlane R., A three color, solid-state three dimensional display, *Science*, 273, 1185-1189, **1996**.
- [14] Watanabe S., Asanuma T., Sasahara T., Hyodo H., Matsumoto M., Soga K., 3D micromolding of arrayed waveguide gratings on upconversion luminescent layers for flexible transparent displays, *Advanced Functional Materials*, 25, 4390-4396, **2015**.
- [15] Meruga J.M., Cross W.M. May, P.S., Luu Q., Crawford G.A., Kellar J.J., Security printing of covert quick response codes using upconverting nanoparticles inks, *Nanotechnology*, 23, 395201-395209, **2012**.
- [16] Ma Q., Wang J., Li Z., Wang D., Hu Z., Zu Y., Yuan Q., Near-infrared light mediated high throughput information encryption based on the inkjet printing of upconversion nanoparticles, *Inorganic Chem. Frontiers*, 4, 1166-1172, **2017**.
- [17] Zhang C., Zhou H.P., Liao L.Y., Wei F., Wei S., Li Z.X., Xu C.H., Fang C.J., Sun L.D., Zhang Y.W., Yan C.H., Luminescence modulation of ordered upconversion nanopatterns by a photochromic diarylethene: rewritable optical storage with nondestructive readout, *Advanced Materials*, 22, 633-637, **2010**.
- [18] Wang F., Liu X., Recent advances in the chemistry of lanthanide-doped upconversion nanocrystals, *Chemical Society Reviews*, 38, 976-989, **2009**.
- [19] Suyver J.F., Aebischer A., Biner D., Gerner P., Grimm J., Heer S., Krämer K., Reinhard C., Güdel H.U., Novel materials doped with trivalent lanthanides and transition metal ions showing near-infrared to visible photon upconversion, *Optical Materials*, 27, 1111-1130, **2005**.
- [20] Suyver J.F., Grimm J., Van Veen M.K., Biner D., Krämer K.W., Güdel H.U., Upconversion spectroscopy and properties of NaYF₄ doped with Er³⁺, Tm³⁺ and/or Yb³⁺, *Journal of Luminescence*, 117, 1-12, **2006**.
- [21] Cotton S., *Lanthanide and actinide chemistry*, Wiley, West Sussex, UK, **2006**.
- [22] Yi G.S., Lu H.C., Zhao S.Y., Ge Y., Yang W.J., Chen D.P., Guo L.H., Synthesis, characterization, and biological application of size-controlled nanocrystalline NaYF₄:Yb,Er infrared-to-visible up-conversion phosphors, *Nano Letters*, 4, 2191-2196, **2004**.
- [23] Boyer J.C., Vetrone F., Cuccia L.A., Capobianco J.A., Synthesis of colloidal upconverting NaYF₄ nanocrystals doped with Er³⁺, Yb³⁺ and Tm³⁺, Yb³⁺ via thermal decomposition of lanthanide trifluoroacetate precursors, *Journal of the American Chemical Society*, 128, 7444-7445, **2006**.
- [24] Zeng J.H., Su J., Li Z.H., Yan R.X., Li Y.D., Synthesis and upconversion luminescence of hexagonal-phase NaYF₄:Yb³⁺, Er³⁺ phosphors of controlled size and morphology, *Advanced Materials*, 17, 2119-2123, **2005**.
- [25] Sivakumar S., Van Veggel F.C.J.M., Raudsepp M., Bright White light through up-conversion of a single NIR source from Sol-gel derived thin film made with Ln³⁺-doped LaF₃ nanoparticles, *Journal of the American Chemical Society*, 127, 12464-12465, **2012**.
- [26] Zhang J., Shen H., Guo W., Wang S., Zhu C., Xue F., Hou J., Su H., Yuan Z., An upconversion NaYF₄:Yb³⁺,Er³⁺/TiO₂ core-shell nanoparticles photoelectrode for improved efficiencies of dye sensitized solar cells, *Journal of Power Sources*, 226, 47-53, **2013**.
- [27] Kongkanand A., Tvrđy K., Takechi K., Kuno M., Kamat P.V., Quantum dot solar cells. Tuning with photoresponse through size and shape control of CdSe-TiO₂ architecture, *Journal of the American Chemical Society*, 130, 4007-4015, **2008**.
- [28] Shan G., Demopoulos G.P. Near infrared sunlight harvesting in dye-sensitized solar cells via the insertion of an upconverter-TiO₂ nanocomposite layer, *Advanced Materials*, 22, 4373-4377, **2010**.
- [29] Li Y., Wang G., Pan K., Jiang B., Tian C., Zhou W., Fu H., NaYF₄:Yb³⁺, Er³⁺-graphene composites: preparation, upconversion luminescence and application in dye sensitized solar cells, *Journal of Materials Chemistry*, 22, 20381-20386, **2012**.
- [30] Tang Y., Di W., Zhai X., Yang R., Qin W., NIR-responsive photocatalytic activity and mechanism of NaYF₄:Yb,Tm@TiO₂ core-shell nanoparticles, *ACS Catalysis*, 3, 405-412, **2013**.
- [31] Lucky S.S., Idris N.M., Li Z., Soo K.C., Zhang Y., Titania coated upconversion nanoparticles for near-infrared light triggered photodynamic therapy, *ACS Nano*, 9, 191-205, **2015**.
- [32] Zhang F., Zhang C.L., Peng H.Y., Cong H.P., Qian H.S., Near-infrared photocatalytic upconversion nanoparticles/TiO₂ nanofibers assembled in large scale by electrospinning, *Particle and Particle Systems Characterizations*, 33, 248-253, **2016**.
- [33] Tong R., Lin H., Chen Y., An N., Wang G., Pan X., Qu F., Near-infrared mediated chemo/photodynamic synergistic therapy with DOX-UCNPs@SiO₂/TiO₂-TC nanocomposites, *Material Science and Engineering C*, 78, 998-1005, **2017**.
- [34] Mavengere S., Kim J.S., UV-Visible light photocatalytic properties of NaYF₄: (Gd, Si)/TiO₂ composites, *Applied Surface Science*, 444, 491-496, **2018**.
- [35] Topel S.D., Cin G.T., Akkaya E.U., Near-IR excitation of heavy atom free photosensitizers through the intermediacy of upconverting nanoparticles, *Chemical Communications*, 50, 8896-8899, **2014**.
- [36] Asilturk M., Sayilkan F., Erdemoglu S., Akarsu M., Sayilkan H., Erdemoglu M., Arpac E., Characterization of the hydrothermally synthesized nano-TiO₂ crystallite and the photocatalytic degradation of Rhodamine B, *Journal of Hazardous Materials*, 129, 164-170, **2006**.
- [37] Mudunkotuwa I.A., Grassian V.H., Citric acid adsorption on TiO₂ nanoparticles in aqueous suspensions at acidic and circumneutral pH: Surface coverage, surface speciation and its impact on nanoparticles-nanoparticle interactions, *Journal of the American Chemical Society*, 132, 14986-14994, **2010**.
- [38] Haase M., Schafer H., Upconverting nanoparticles, *Angewandte Chemie International Edition*, 50, 5808-5829, **2011**.
- [39] Yu X., Li M., Chen L., Li Y., Wang Q., Dopant-controlled synthesis of water-soluble hexagonal NaYF₄ nanorods with efficient upconversion fluorescence for multicolor Bioimaging, *Nano Research*, 3, 51-60, **2010**.
- [40] Joint Committee on Powder Diffraction Standards, Diffraction Data File No. 21-1272 International Center for Diffraction Data, Pennsylvania.
- [41] Lü Q., Zhao L.C., Guo F.Y., Li M.C., Upconversion emission enhancement of TiO₂ coated lanthanide-doped Y₂O₃ nanoparticles. *Chinese Physics B*, 18, 4030-4036, **2009**.

6. ACKNOWLEDGEMENTS

The authors acknowledge the Akdeniz University Coordination Unit of Scientific Research Projects (Project No. 2012.01.0115.001) for their financial support. Authors also thank Prof. Engin U. Akkaya (Department of Chemistry, Bilkent University, Ankara, Turkey) for his help and support and Mr. Mustafa Guler (UNAM, Bilkent University, Ankara, Turkey) for TEM imaging.

© 2018 by the authors. This article is an open access article distributed under the terms and conditions of the Creative Commons Attribution license (<http://creativecommons.org/licenses/by/4.0/>).